

This is a self-archived version of an original article. This version may differ from the original in pagination and typographic details.

Author(s): Zhu, Qihao; Fettinger, James C.; Vasko, Petra; Power, Philip P.

Title: Interactions of a Diplumbyne with Dinuclear Transition Metal Carbonyls to Afford Metalloplumbylenes

Year: 2020

Version: Accepted version (Final draft)

Copyright: © 2020 American Chemical Society

Rights: In Copyright

Rights url: <http://rightsstatements.org/page/InC/1.0/?language=en>

Please cite the original version:

Zhu, Q., Fettinger, J. C., Vasko, P., & Power, P. P. (2020). Interactions of a Diplumbyne with Dinuclear Transition Metal Carbonyls to Afford Metalloplumbylenes. *Organometallics*, 39(24), 4629-4636. <https://doi.org/10.1021/acs.organomet.0c00659>

Interactions of a Diplumbyne with Dinuclear Transition Metal Carbonyls to Afford Metalloplumbylenes

Qihao Zhu, Petra Vasko, James C. Fettinger, and Philip P. Power*

Abstract:

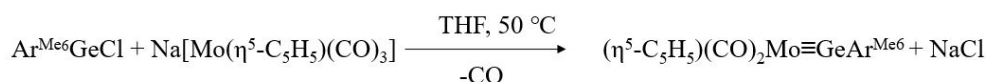
The metathesis reactions of the diplumbyne $\text{Ar}^{\text{iPr}_6}\text{PbPbAr}^{\text{iPr}_6}$ ($\text{Ar}^{\text{iPr}_6} = -\text{C}_6\text{H}_3-2,6-(\text{C}_6\text{H}_2-2,4,6-\text{iPr}_3)_2$) with the dinuclear metal carbonyls $\text{Mn}_2(\text{CO})_{10}$, $\text{Fe}_2(\text{CO})_9$, $\text{Co}_2(\text{CO})_8$ under mild conditions afforded the complexes $\text{Mn}(\text{CO})_5(\text{PbAr}^{\text{iPr}_6})$ (**1**), $\text{Fe}(\text{CO})_4(\text{PbAr}^{\text{iPr}_6})_2$ (**2**), $\text{Co}_4(\text{CO})_9(\text{PbAr}^{\text{iPr}_6})_2$ (**3**), respectively. Complexes **1-3** were structurally characterized by single-crystal X-ray diffraction, and by ^1H , $^{13}\text{C}\{^1\text{H}\}$, $^{59}\text{Co}\{^1\text{H}\}$, and $^{207}\text{Pb}\{^1\text{H}\}$ NMR, UV-Vis, and IR spectroscopy. They are rare examples of species formed by the direct reaction of a group 14 dimetallene with transition metal carbonyls. Complexes **1** and **2** feature Mn-Pb or Fe-Pb single bonds whereas in **3** a Co-Pb cluster is formed in which the plumbylidyne moiety bridges either an edge or a face of a Co_4 carbonyl cluster.

Introduction

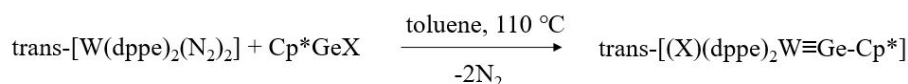
Organometallic complexes containing bonds between transition metals and low oxidation state group 14 element moieties are of interest because of their potential for a diverse reactivity thus arises mainly from the unsaturated character of the group 14 element bound directly to the transition metal.¹ For the heavier group 14 elements, early work by Marks² and Lappert³ reported the synthesis of the first stannylene-transition metal complexes which were characterized spectroscopically²⁻³ and structurally.³ These initial examples have been followed by numerous other L_nMER_2 (L = ligand; M = transition metal; E = heavier group 14 element; R = organic & related substituents)

complexes that have incorporated the other heavier group 14 elements and various transition metals.⁴⁻⁶ Related to these complexes are species of formula L_nM-ER in which the transition metal is σ -bonded directly to the group 14 element. The first such complex, $Mes^*GeFe(CO)_2R$ (Mes^* = supermesityl, i.e. $C_6H_2-2,4,6-^tBu_3$; $R = Cp/Cp^*$), which was reported by Jutzi and Leue in 1994, was characterized spectroscopically.⁷ Later Power and coworkers reported the synthesis of metallostannylenes⁸, $Cp(CO)_3MSnAr^{Me6}$, and metalloplumbylenes⁹, $Cp(CO)_3MSnAr^{iPr6}$ ($M = Cr, Mo, \text{ or } W$; $Ar^{Me6} = -C_6H_3-2,6-(C_6H_2-2,4,6-Me_3)_2$; $Ar^{iPr6} = -C_6H_3-2,6-(C_6H_2-2,4,6-^iPr_3)_2$), analogues, and related species¹⁰. Attempts to generate the corresponding metallogermylenes led to the fortuitous discovery of a metallogermylyne featuring a molybdenum-germanium triple bond¹¹ via carbon monoxide elimination (Scheme 1). In contrast, the corresponding chemistry with the chromium or tungsten species afforded several examples of the desired singly bonded metallogermylenes.¹² Work by Filippou and coworkers disclosed other routes to the metallogermylynes¹³ and metallogermylenes (Scheme 1) and expanded their results to include the corresponding complexes with triple bonds to tin¹⁴ and lead.¹⁵

*Power et. al*¹¹



*Filippou et. al*¹³



$X = \text{halide}; Ar^{Me6} = -C_6H_3-2,6-(C_6H_2-2,4,6-Me_3)_2$
 $Cp^* = C_5Me_5$; $dppe = Ph_2PCH_2CH_2PPh_2$

Scheme 1. Synthetic routes to metallogermylynes.

More recent work¹⁶ has shown that the above species can be synthesized by metathesis

of the dimetallynes REER (R = terphenyl; E = Ge,¹⁷ Sn,¹⁸ or Pb¹⁹) with the single or triple bonded transition metal species, (CO)₃CpMo-MoCp(CO)₃ or (CO)₂CpMo≡MoCp(CO)₂.¹⁶ In addition, the distannyne and digermynes were reacted with the group 6 carbonyls M(CO)₆ to form the cluster species, {Ar^{iPr4}EM(CO)₄}₂ (E = Ge, Sn; Ar^{iPr4} = -C₆H₃-2,6-(C₆H₃-2,6-ⁱPr₃)₂).²⁰ However, the reactivity of diplumbynes towards simple transition metal carbonyls remains hardly explored. Herein, we report the syntheses and characterizations of metalloplumbylenes Mn(CO)₅(PbAr^{iPr6}) (**1**), Fe(CO)₄(PbAr^{iPr6})₂ (**2**), Co₄(CO)₉(PbAr^{iPr6})₂ (**3**) by reactions of the diplumbyne, Ar^{iPr6}PbPbAr^{iPr6}, with the dinuclear metal carbonyls, Mn₂(CO)₁₀, Fe₂(CO)₉, Co₂(CO)₈.

Experimental Section

General Procedures. All operations were carried out by using modified Schlenk techniques or in a Vacuum Atmospheres OMNI-Lab drybox under an atmosphere of dry argon or nitrogen. The lead compounds were manipulated with careful exclusion of light due to the tendency of low-valent lead compounds to decompose or disproportionate under illumination. Solvents were dried over an alumina column and degassed prior to use.²¹ The compound Ar^{iPr6}PbPbAr^{iPr6} was prepared according to literature procedures.^{19, 22} Metal carbonyls were used as purchased without further purification. Na[Mn(CO)₅] was prepared by a modified literature procedure (see SI).²³⁻
²⁵ The ¹H, ¹³C{¹H}, ⁵⁹Co{¹H}, and ²⁰⁷Pb{¹H} NMR spectra were recorded on a Varian Inova 600 MHz spectrometer. The ¹H and ¹³C{¹H} NMR spectra were referenced to the residual solvent signals in C₆D₆. The ⁵⁹Co{¹H} NMR spectrum was referenced to an

external standard of a saturated solution of $\text{K}_3\text{Co}(\text{CN})_6$ (δ 0.0 ppm) in D_2O . The $^{207}\text{Pb}\{^1\text{H}\}$ NMR spectra were referenced to an external standard of PbMe_4 (δ 0.0 ppm) in CDCl_3 . UV-Visible spectra were recorded in dilute hexane solutions in 3.5 mL quartz cuvettes using an Olis 17 Modernized Cary 14 UV-Vis/NIR spectrophotometer. Infrared spectra were collected on a Bruker Tensor 27 ATR-FTIR spectrometer.

$\text{Mn}(\text{CO})_5(\text{PbAr}^{\text{iPr}_6})$ (1). Method A: ca. 50 mL of THF were added to a heavy-walled Teflon tapped Schlenk flask charged with 0.395 g (0.29 mmol) $\text{Ar}^{\text{iPr}_6}\text{PbPbAr}^{\text{iPr}_6}$ and 0.122 g (0.31 mmol) $\text{Mn}_2(\text{CO})_{10}$. The flask was then sealed, and the solution was stirred at ambient temperature for 2 days, and then heated to ca. 50 °C for 5 days, during which time the color changed from dark brown to dark green. The solution was cooled to room temperature, and filtered. The solution was then concentrated under reduced pressure to ca. 10 mL, and cooled to a ca. -18 °C for one week to afford the product as teal crystals of $\text{Mn}(\text{CO})_5(\text{PbAr}^{\text{iPr}_6})$ (1). Yield: 0.098 g, 19 %.

Method B: 0.46 g (2.11 mmol) $\text{Na}[\text{Mn}(\text{CO})_5]$ in ca. 40 mL Et_2O solution was added dropwise over 15 minutes to a Schlenk flask charged with 1.472 g (0.96 mmol) $[\text{Ar}^{\text{iPr}_6}\text{Pb}(\mu\text{-Br})]_2$ and ca. 30 mL of Et_2O at 0 °C,. After stirring for 2 days, during which time the color changed from yellow to teal, solvent was removed and the residue was extracted with hexanes, and filtered. The hexanes were removed under reduced pressure and ca. 20 mL of Et_2O was added. Storage of the solution at room temperature overnight afforded teal crystals of $\text{Mn}(\text{CO})_5(\text{PbAr}^{\text{iPr}_6})$ (1) that were suitable for X-ray diffraction studies. Yield: 1.392 g, 82 %. ^1H NMR (600 MHz, C_6D_6 , 298K, ppm): δ = 1.09 (br,

12H, p-CH(CH₃)₂), 1.19 (d, 12H, o-CH(CH₃)₂), ³J_{H,H} = 6.6 Hz, 1.38 (d, 12H, o-CH(CH₃)₂), ³J_{H,H} = 6.6 Hz, 2.77 (sept, 2H, p-CH(CH₃)₂), ³J_{H,H} = 7.2 Hz, 3.40 (br, 4H, o-CH(CH₃)₂) ³J_{H,H} = 5.8 Hz; 7.12 (br, 4H, m-Trip); 7.55 (t, 1H, p-C₆H₃) ³J_{H,H} = 7.3 Hz, 8.03 (d, 2H, m-C₆H₃) ³J_{H,H} = 7.3 Hz. ¹³C{¹H} NMR (151 MHz, C₆D₆, 298K, ppm): δ = 23.54 (o-CH(CH₃)₂), 23.95 (o-CH(CH₃)₂), 27.44 (p-CH(CH₃)₂), 30.90 (o-CH(CH₃)₂), 34.78 (p-CH(CH₃)₂), 122.49 (br, m-Trip), 125.30 (p-C₆H₃), 128.30 (m-C₆H₃), 133.02 (i-Trip), 140.54 (p-Trip), 146.38 (o-Trip), 149.17 (o-C₆H₃), 210.94 (br, CO), 282.93 (br, CO). ²⁰⁷Pb{¹H} NMR (125 MHz, C₆D₆, 298K, ppm): δ = 8007.2. ATR-FTIR: ν_{CO} (cm⁻¹): 1958(s), 2060(m). UV-vis (hexane) λ_{max} = nm (ε = M⁻¹·cm⁻¹): 332 (13700), 671 (1640).

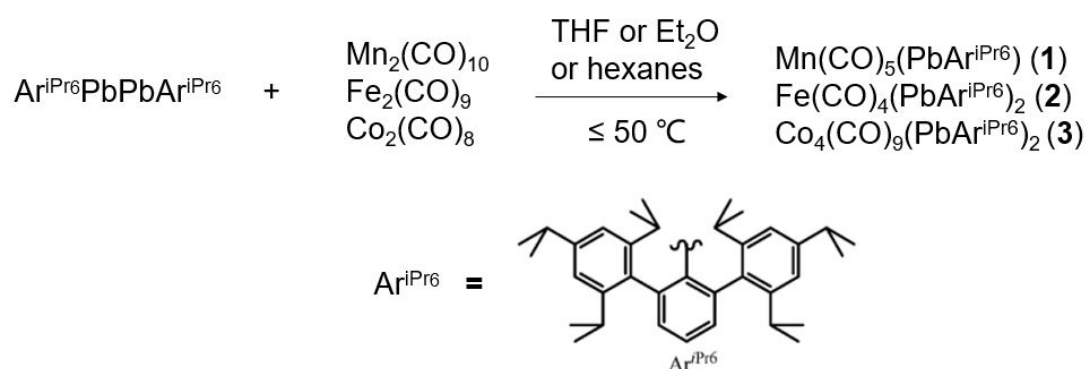
Fe(CO)₄(PbAr^{iPr6})₂ (2). ca. 50 mL of Et₂O was added to a Schlenk flask charged with 0.452 g (0.33 mmol) Ar^{iPr6}PbPbAr^{iPr6} and 0.132 g (0.36 mmol) Fe₂(CO)₉. The solution was stirred for 2 days, during which time the color changed from dark brown to green. The solution was filtered, concentrated under reduced pressure to ca. 10 mL, and cooled to ca. -18 °C for one week to afford crystals of Fe(CO)₄(PbAr^{iPr6})₂ (**2**) as green needles that were suitable for X-ray diffraction studies. Yield: 0.295 g, 58 %. ¹H NMR (600 MHz, C₆D₆, 298K, ppm): δ = 1.13 (d, 12H, p-CH(CH₃)₂), ³J_{H,H} = 5.5 Hz. 1.28 (d, 12H, o-CH(CH₃)₂), ³J_{H,H} = 6.2 Hz, 1.36 (d, 12H, o-CH(CH₃)₂), ³J_{H,H} = 7.0 Hz, 2.85 (sept, 2H, p-CH(CH₃)₂), ³J_{H,H} = 6.6 Hz, 3.46 (broad, 4H, o-CH(CH₃)₂) ³J_{H,H} = 5.8 Hz; 7.12 (s, 4H, m-Trip); 7.51 (t, 1H, p-C₆H₃) ³J_{H,H} = 7.1 Hz, 8.06 (d, 2H, m-C₆H₃) ³J_{H,H} = 7.9 Hz. ¹³C{¹H} NMR (151 MHz, C₆D₆, 298K, ppm): δ = 23.46 (o-CH(CH₃)₂), 24.24 (o-CH(CH₃)₂), 27.14 (p-CH(CH₃)₂), 30.66 (o-CH(CH₃)₂), 34.73 (p-CH(CH₃)₂), 120.73 (m-Trip), 124.99 (p-C₆H₃), 128.29 (m-C₆H₃), 133.60 (i-Trip), 141.21 (p-Trip), 145.95

(o-Trip), 149.00 (o-C₆H₃), 295.48 (br, CO). ²⁰⁷Pb{¹H} NMR (125 MHz, C₆D₆, 298K, ppm): not observed. ATR-FTIR: ν_{CO} (cm⁻¹): 1889(m), 1958(m), 2005(m), 2041(w). UV-vis (hexane) λ_{max} = nm (ϵ = M⁻¹·cm⁻¹): 341 (22700), 505 (3140), 641 (3000).

Co₄(CO)₉(PbAr^{iPr6})₂ (3). ca. 50 mL of hexane was added to a Schlenk flask charged with 0.330 g (0.24 mmol) Ar^{iPr6}PbPbAr^{iPr6} and 0.168 g (0.49 mmol) Co₂(CO)₈. After stirring overnight, during which time the color changed from dark brown to dark red, the solution was filtered, concentrated under reduced pressure to ca. 15 mL, and cooled to ca. -30 °C for one week to afford crystals of Co₄(CO)₉(PbAr^{iPr6})₂ (**3**) as dark maroon blocks that were suitable for X-ray diffraction studies. Yield: 0.299 g, 67 %. ¹H NMR (600 MHz, C₆D₆, 298K, ppm): δ = 1.11 (d, 12H, p-CH(CH₃)₂), ³J_{H,H} = 6.6 Hz. 1.38 (d, 12H, o-CH(CH₃)₂), ³J_{H,H} = 6.9 Hz, 1.56 (d, 12H, o-CH(CH₃)₂), ³J_{H,H} = 6.9 Hz, 2.92 (sept, 2H, p-CH(CH₃)₂), ³J_{H,H} = 7.1 Hz, 3.16 (broad, 4H, o-CH(CH₃)₂) ³J_{H,H} = 7.4 Hz; 7.26 (s, 4H, m-Trip); 7.38 (t, 1H, p-C₆H₃) ³J_{H,H} = 5.9 Hz, 7.88 (d, 2H, m-C₆H₃) ³J_{H,H} = 7.3 Hz. ¹³C{¹H} NMR (151 MHz, C₆D₆, 298K, ppm): δ = 23.47 (o-CH(CH₃)₂), 24.05 (o-CH(CH₃)₂), 26.14 (p-CH(CH₃)₂), 31.08 (o-CH(CH₃)₂), 34.92 (p-CH(CH₃)₂), 123.15 (m-Trip), 128.89 (p-C₆H₃), 134.74 (m-C₆H₃), 138.52 (i-Trip), 143.57 (p-Trip), 146.42 (o-Trip), 149.99 (o-C₆H₃), 213.17 (br, CO). ⁵⁹Co NMR (142 MHz, C₆D₆, 298K, ppm): δ = -173.0 (Co(1), relative intensity = 1), -654.4 (Co(2) and Co(3), relative intensity = 2), -2016.0 (Co(4), relative intensity = 1). ²⁰⁷Pb{¹H} NMR (125 MHz, C₆D₆, 298K, ppm): δ = 9010.4. ATR-FTIR: ν_{CO} (cm⁻¹): 1820(m), 1849(m), 1948(m), 1972(s), 2008(m), 2035(m). UV-vis (hexane) λ_{max} = nm (ϵ = M⁻¹·cm⁻¹): 368 (shoulder, 57700).

Results and Discussion

Synthesis. Metathetical exchange between group 14 dimetallynes, $\text{Ar}^{\text{iPr}_6}\text{MMAr}^{\text{iPr}_4}$ or $\text{Ar}^{\text{iPr}_6}\text{MMAr}^{\text{iPr}_6}$ ($\text{M} = \text{Ge}, \text{Sn}, \text{or Pb}$) and $(\text{CO})_3\text{CpMo-MoCp}(\text{CO})_3$ or $(\text{CO})_2\text{CpMo}\equiv\text{MoCp}(\text{CO})_2$, was shown earlier to afford the complexes, $\text{Ar}^{\text{iPr}_4}\text{M}\equiv\text{MoCp}(\text{CO})_2$, $\text{Ar}^{\text{iPr}_6}\text{M}\equiv\text{MoCp}(\text{CO})_2$, and $\text{Ar}^{\text{iPr}_4}\text{M-MoCp}(\text{CO})_3$ or $\text{Ar}^{\text{iPr}_6}\text{M-MoCp}(\text{CO})_3$.¹⁶ In particular, the relatively weak Pb-Pb bond of the diplumbyne²² is expected to facilitate these reactions with metal-metal (M-M) bonded transition metal carbonyl dimers, hence we studied the reactions of the nominally M-M bonded dinuclear metal carbonyls $\text{Mn}_2(\text{CO})_{10}$, $\text{Fe}_2(\text{CO})_9$, $\text{Co}_2(\text{CO})_8$ with the diplumbyne, $\text{Ar}^{\text{iPr}_6}\text{PbPbAr}^{\text{iPr}_6}$. Compounds $\text{Mn}(\text{CO})_5(\text{PbAr}^{\text{iPr}_6})$ (**1**), $\text{Fe}(\text{CO})_4(\text{PbAr}^{\text{iPr}_6})_2$ (**2**), $\text{Co}_4(\text{CO})_9(\text{PbAr}^{\text{iPr}_6})_2$ (**3**) were attained by the reaction of the diplumbyne with the dinuclear metal carbonyls either in ethereal solvents (Et_2O or THF) or in hexanes (Scheme 2). For compounds **2** and **3**, the syntheses were carried at ambient temperature, and the products were isolated in moderate to good yields. A similar approach to the



Scheme 2. Reactions of $\text{Ar}^{\text{iPr}_6}\text{PbPbAr}^{\text{iPr}_6}$ with metal carbonyls.

synthesis of **1** afforded a color change from dark brown to green. However, the major signals in the ^1H NMR spectrum of the residue after removal of solvent were attributed

to the unreacted starting materials. To avoid the propensity for decomposition of the diplumbyne under irradiation, gentle heating was applied to the reaction solution after stirring at room temperature for two days. This approach afforded **1** in low (ca. 20%) yield. In contrast, an alternative approach to the synthesis of **1** via salt metathesis of $[\text{Ar}^{\text{iPr}_6}\text{Pb}(\mu\text{-Br})]_2$ and $\text{Na}[\text{Mn}(\text{CO})_5]$ afforded **1** in a much higher (82%) yield.

The synthesis of **1** by reaction of $\text{Ar}^{\text{iPr}_6}\text{PbPbAr}^{\text{iPr}_6}$ and $\text{Mn}_2(\text{CO})_{10}$ is formally a metathetical exchange between the $\text{Pb}\equiv\text{Pb}$ 'triple' bond and the Mn-Mn single bond. However, for steric reasons it seems unlikely that this reaction proceeds via intact dinuclear metal carbonyls. In the cases of **1-3**, it is proposed that the diplumbyne, $\text{Ar}^{\text{iPr}_6}\text{PbPbAr}^{\text{iPr}_6}$, dissociates into $\text{Ar}^{\text{iPr}_6}\text{Pb}\cdot$ radical fragment^{16, 26}, followed by subsequent reaction with $\text{Mn}_2(\text{CO})_{10}$, $\text{Fe}_2(\text{CO})_9$, or $\text{Co}_2(\text{CO})_8$.

The yields of the reactions between diplumbyne and metal carbonyls are possibly affected by the transition metal-metal (M-M) bond strength. Recently, Shaik and coworkers presented computational studies on the M-M bonds in transition metal complexes using of ab initio valence-bond methods, in which the M-M bonds of the 3d-series (group 3-10) are considered as pure charge shift bonds.²⁷ The Mn-Mn bond in $\text{Mn}_2(\text{CO})_{10}$ is calculated to have a bond dissociation energy of 22.9 kcal/mol with a charge-shift resonance energy of 24.5 kcal/mol (experimental 38.0 ± 5 kcal/mol)²⁸ suggesting that the Mn-Mn bond is the strongest M-M bond among $\text{Mn}_2(\text{CO})_{10}$,²⁷ $\text{Fe}_2(\text{CO})_9$ (no Fe-Fe bond),²⁹ and $\text{Co}_2(\text{CO})_8$ (9.8 kcal/mol),²⁷ which may account for the relatively low yield of **1** in the reaction between $\text{Ar}^{\text{iPr}_6}\text{PbPbAr}^{\text{iPr}_6}$ and $\text{Mn}_2(\text{CO})_{10}$.

Both the teal crystals of **1**, and green crystals of **2** are highly air-sensitive, and an

immediate color change is observed upon their exposure to air. Dark maroon crystals of **3** can be briefly handled in air without displaying significant color change. Hydrocarbon solutions of **1**, **2**, and **3** were prone to decomposition by light over time, with lead metal deposition and a lightening of the color of the solution.

Structures. The solid-state molecular structures of compounds **1**, **2**, and **3** were determined by single crystal X-ray crystallography. Selected bond distances and bond angles are given in Table 1, and the molecular structures of **1**, **2**, and **3** are illustrated in Figures 1-3, respectively.

Compound **1** crystallized in the $I2/a$ space group. The manganese atom in compound **1** is six-coordinate with a near-octahedral coordination geometry. The Pb-Mn distance is 2.838(4) Å, which is slightly longer than the Pb-Mn single bonds in $[Pb\{Mn(CO)_5\}_3][AlCl_4]$ ³⁰ (2.750(1)-2.785(1) Å), and the Pb-Mn single bond in the dimetalloborylene complex, $(Ph_3Pb)[Mn(\eta^5-C_5H_5)(CO)_2]_2B$, 2.703(7) Å.³¹ The Pb-Mn bond distance in **1** is slightly shorter than the sum (2.85 Å) of the covalent radii of Mn(1.39 Å) and Pb(1.46 Å).³²⁻³⁴ The interligand angles at the Mn atom range from 82.65(8)° to 96.75(11)° which deviate somewhat (<7.5°) from the 90° value expected for idealized octahedral coordination. The C(1)-Pb(1)-Mn(1) angle at the lead atom is 106.45(5)°.

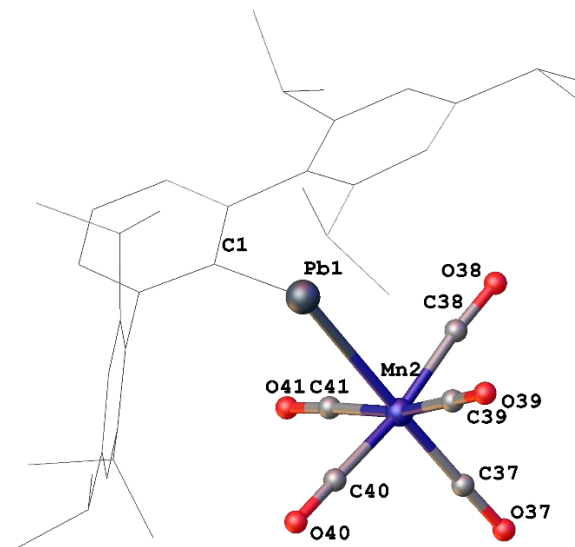


Figure 1. Thermal ellipsoid (50%) plot of **1**. H atoms and disordered groups are not shown for clarity, the organic substituents are shown as wire frames.

The molecular structure of **2** showed that it has a six-coordinated iron atom with four carbonyl ligands and two mutually *cis*-PbAr^{iPr6} moieties, which afford distorted octahedral coordination at iron. The interligand angles at the iron atom range from 75.0(5)° to 106.5(7)°. The deviation of interligand angles from ideal octahedral geometry at iron is possibly due to the steric hindrance between the two *cis*-PbAr^{iPr6} moieties. The two Pb-Fe bond distances are 2.830(3) Å, and 2.804(3) Å, which are slightly longer than the sum (2.78 Å) of the covalent radii of Pb(1.46 Å) and Fe(1.32 Å).³²⁻³⁴ The Pb-Fe bond lengths in **2** are slightly longer than the Pb-Fe distances, (2.736(2) Å and 2.728(2) Å), observed in [Et₂PbFe(CO)₄]₂ by Wrackmeyer and coworkers.³⁵ The relatively long Fe-Pb and Mn-Pb distances in **1** and **2** are consistent

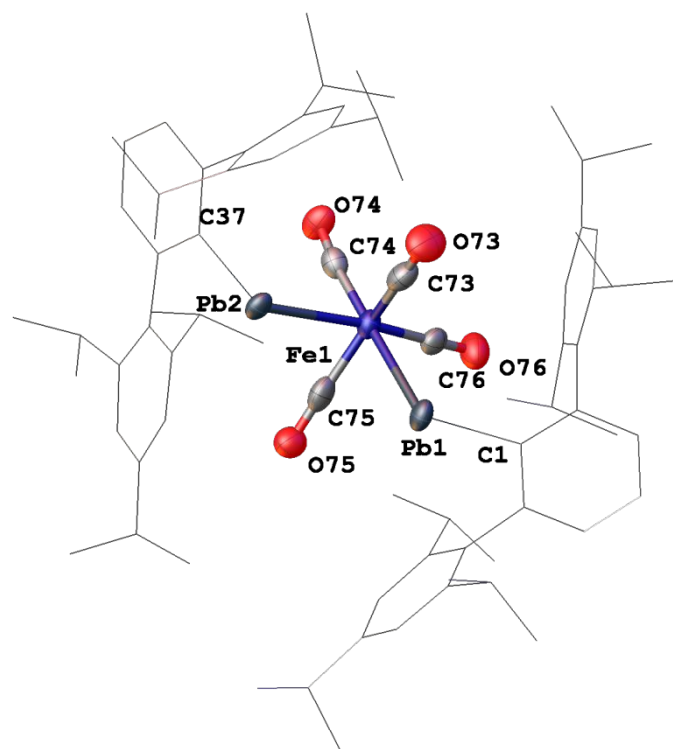


Figure 2. Thermal ellipsoid (50%) plot of **2**. H atoms and disordered groups are not shown for clarity, the organic substituents are shown as wire frames.

with a +2 oxidation state of lead as the σ -bonds are likely to be dominated by the p-orbital character from the Pb(II) atom, assuming that the transition metal carbonyl fragment carries a negative charge.⁹ The interligand angles at the lead atom(s) of **1** ($106.45(5)^\circ$) and **2** ($100.50(3)^\circ$, $102.70(3)^\circ$) are slightly narrower than those in the $\text{Cp}(\text{CO})_3\text{M-PbAr}^{\text{iPr}_6}$ ($\text{M}=\text{Cr}, \text{Mo}, \text{W}$) complexes ($108.6(2)^\circ$ - $113.58(9)^\circ$),⁹ possibly due to the steric differences between carbonyl groups and cyclopentadienyl group. The structures of **1** and **2** can also be rationalized by the 18-electron rule where the $\text{PbAr}^{\text{iPr}_6}$ moieties are 1-electron ligands bound to the transition metals.⁹

Compound **3** crystallized as dark maroon blocks in the $\text{P2}_1/\text{c}$ space group. The molecular structure of **3** displays a near-tetrahedral Co_4 core bonded to a total of nine

carbonyls and two $\text{PbAr}^{\text{iPr}_6}$ moieties. Seven of the carbonyls are terminally bound, with the remaining two carbonyls and one of the $\text{PbAr}^{\text{iPr}_6}$ moieties each bridging one of the three edges linking the apical cobalt atom with the three basal cobalt atoms. The remaining $\text{PbAr}^{\text{iPr}_6}$ moiety bridges the face formed from the three basal cobalt atoms. The apical cobalt atom carries only one terminal carbonyl, while each of the basal cobalt atoms carry two terminal carbonyls. The structure of **3** therefore differs from that of $\text{Co}_4(\text{CO})_{12}$, where the apical atom is connected to three terminal carbonyls. The structure of compound **3** conforms to Wade's rules which predict a *nido* structure for the tetracobalt tetrahedron core as it has $n+2$ (n =no. of vertices) skeletal electron pairs

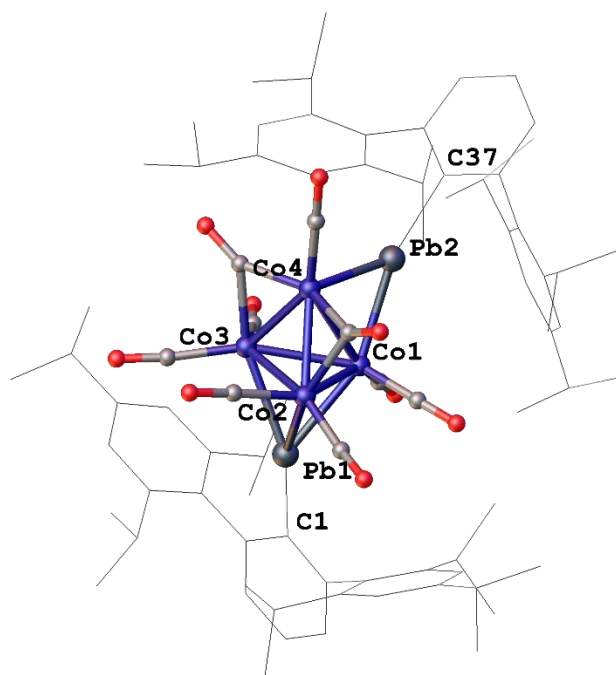


Figure 3. Thermal ellipsoid (50%) plot of **3**. H atoms and disordered groups are not shown for clarity, the organic substituents are shown as wire frames.

for cluster bonding.³⁶⁻³⁷ The edge-bridging Pb-Co bonds are 2.5008(7) Å and 2.5150(6) Å, while the average of the face-bridging Pb-Co distances is 2.5750(8) Å, which is

Table 1. Selected bond distances (Å) and angles (°) for **1-3**.

	1 (M = Mn)	2 (M = Fe)	3 (M = Co)
Pb-C	2.288(2)	Pb(1)-C(1) 2.313(13) Pb(2)-C(37) 2.307(13)	Pb(1)-C(1) 2.229(2) Pb(2)-C(37) 2.214(2)
Pb-M	2.8376(4)	Pb(1)-Fe(1) 2.800(2) Pb(2)-Fe(1) 2.829(2)	2.5078(4) (average of edge-bridging) 2.5735(4) (average of face-bridging)
M-CO (average)	1.839(3)	1.772(19)	1.775(3) (terminal) 1.932(3) (bridging)
M-Pb-C	106.45(5)	C(1)-Pb(1)-Fe(1) 102.70(3) C(37)-Pb(2)-Fe(1) 100.50(3)	C(37)-Pb(2)-Co(4) 130.44(7) C(37)-Pb(2)-Co(1) 162.43(7) (edge-bridging) C(1)-Pb(1)-Co(1) 128.18(6) C(1)-Pb(1)-Co(2) 153.22(6) C(1)-Pb(1)-Co(3) 146.90(6) (face-bridging)

slightly longer than the edge-bridging distance as expected for the higher coordination number. The Co-Co lengths are similar to those of the Co-Co bonds (2.441(14) Å to 2.527(10) Å) in cobalt carbonyl clusters³⁸ except that the Co(1)-Co(4) distance bridged by the PbAr^{iPr6} moiety which is 2.7472(9) Å, much longer than an average Co-Co bond, 2.499(1) Å.³⁹⁻⁴¹ The calculated structure of the unsaturated compound Co₄(CO)₁₁ reported by King and coworkers⁴² was predicted to have a μ₄-CO group bridging all four cobalt atoms, where the structure of **3** resembles one of the predicted structures with a butterfly array of cobalt atoms. The calculated structure indicated a long Co···Co distance between the two wingtips cobalt atoms of 2.974 Å (B3LYP) or 3.105 Å (BP86), in the Co₄ butterfly, 0.2~0.3 Å longer than Co(1)-Co(4) in the structure of **3**.⁴² The structure of **3** displays wide interligand angles at the lead atoms (see Table 1) thus arises from the bridging nature of the PbAr^{iPr6} moieties and the higher coordination number

at lead atom. In addition, the sum of the angles at Pb(2) is 359.26(7)°, consistent with a planar coordination geometry. The Pb-C distances in **1-3** range from 2.214(2) Å to 2.313(13) Å which are within the range of reported divalent aryllead species.⁴³⁻⁴⁵ The transition metal-carbon distances to the carbonyl groups are comparable to their parent metal carbonyls.⁴⁶

Spectroscopy. ¹H and ¹³C{¹H} NMR spectra of **1**, **2**, and **3** indicate the high purity of the samples. The ¹H NMR spectra of **1** and **2** each displayed a set of signals which correspond to the ligand, Ar^{iPr6}.⁴⁵ Peak broadenings were observed in the ¹H NMR spectrum of **1** possibly due to restricted rotations of the flanking rings, which has been noted previously.²² The ¹H NMR spectrum of **3** displayed two sets of peaks attributable to the ligand which differ by approximately 0.01 ppm due to the two slightly different environments of the face-bridging and edge-bridging lead atoms.

The ¹³C{¹H} NMR spectra of **1**, **2**, and **3** displayed signals similar to those in the previously reported complexes, (η⁵-C₅H₅)(CO)₃M-PbAr^{iPr6} (M=Cr, Mo, W), including **3** where there was only one set of signals from the ligand, Ar^{iPr6}. The ¹³C{¹H} NMR spectrum of **1** displayed two peaks attributable to the carbonyl groups at 210.94 ppm, and 282.93 ppm (Table 2) in an approximate integration ratio of 4:1, which correspond to the COs cis and trans to the PbAr^{iPr6} substituents. There is no indication of restricted rotation around the Pb(1)-Mn(1) axis in the ¹³C{¹H} NMR spectrum, consistent with a single bond between Pb and Mn. The ¹³C{¹H} NMR spectra of **2** and **3** each showed a single broad signal at 295.48 ppm, and 213.17 ppm for the carbonyl groups, respectively. (see Table 2) The ¹³C{¹H} NMR spectrum of **2** can be understood by

having an overall C_{2v} symmetry for its solid-state structure. It is unclear of missing signals in the $^{13}C\{^1H\}$ NMR spectrum of **3**, where it has been previously reported of missing apical ^{13}C signal in the $^{13}C\{^1H\}$ NMR spectrum of $Co_4(CO)_{12}$.⁴⁷

The $^{207}Pb\{^1H\}$ NMR spectra of **1** and **3** displayed broad signals at 8007.2 ppm, and 9010.4 ppm (Table 2) which are in fair agreement with ^{207}Pb NMR signals observed for $(\eta^5-C_5H_5)(CO)_3M-PbAr^{iPr_6}$ ($M=Cr, Mo, W$), 9374-9659 ppm,⁹ are also the chemical shift range for two-coordinated lead.⁴⁴ Signal broadening in $^{207}Pb\{^1H\}$ NMR spectrum of **3** could be caused by coupling to multiple ^{59}Co atoms as ^{59}Co is a 7/2 spin nucleus and thus quadrupolar.⁴⁸ The $^{59}Co\{^1H\}$ NMR spectrum of **3** displayed three signals at -173.0 ppm, -654.4 ppm, and -2016.0 ppm, respectively. The intensity ratio of the three signals is 1:2:1 which corresponds to the three different chemical environments for the cobalt atoms seen in the crystal structure of **3**. The chemical shifts in the ^{59}Co NMR spectrum of tetrahedral clusters supported by carbonyl ligands are generally unaffected by edge-bridging or face-bridging metals.⁴⁸ The signal at -173.0 ppm can be assigned to Co(1), the more intense signal at -654.4 ppm can be assigned to both Co(2) and Co(3) where Co(1), Co(2) and Co(3) are all bonded to two terminal carbonyl ligands in its solid state, and the signal at -2016.0 ppm to Co(4), which is bonded to two bridged carbonyl ligands and one terminal carbonyl ligand, respectively, suggesting that solid-state structure of **3** is also present in the solution structure. The chemical shifts of the signals are close to those chemical shifts reported for $Co_4(CO)_{12}$, -668 ppm (apical Co), and -2032 ppm (basal Co) in $CDCl_3$.⁴⁸

The UV-vis spectra of **1** and **2** showed absorptions at 671 nm and 641 nm (Table 2),

respectively, which are attributed to the n-p transitions of the lead atoms as depicted in DFT calculations (Figure 4). These absorptions are close to the reported values for (η^5 -C₅H₅)(CO)₃M-PbAr^{iPr}₆ 611-624 nm.⁹ However, the UV-vis spectrum of **3** displayed an absorption at 368 nm that is blue-shifted compared to absorptions of plumbylenes, possibly due to the large extinction coefficient of cobalt-centered electronic transition where the absorption is very similar to what was reported for Co₄(CO)₁₂ (372 nm).⁴⁹

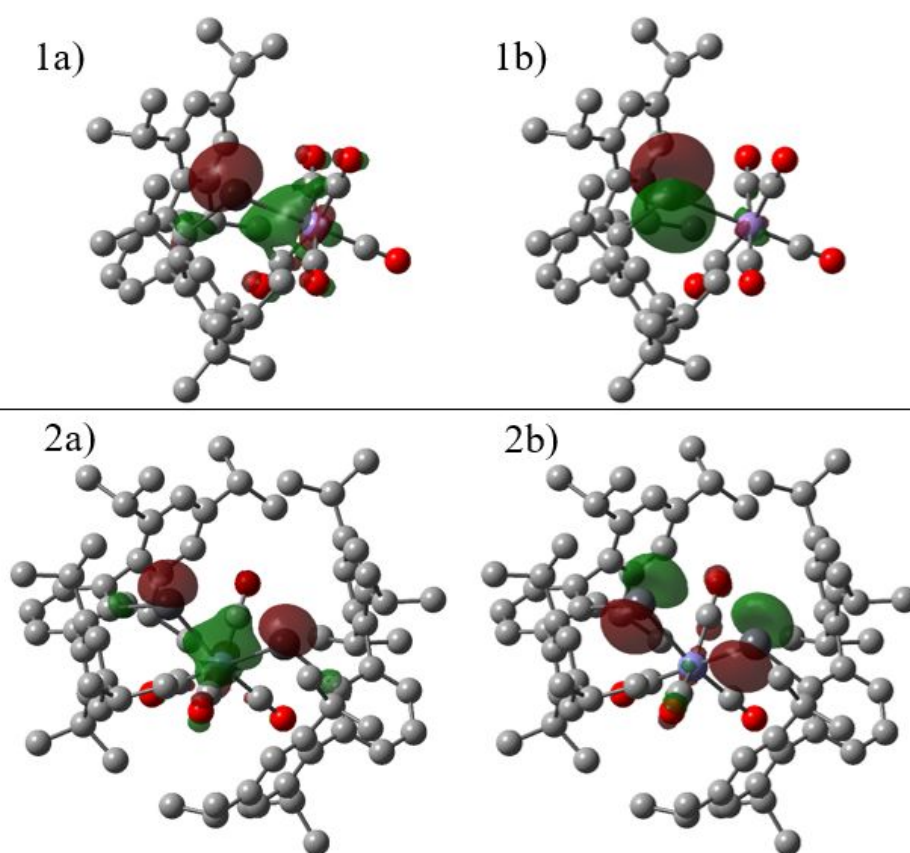


Figure 4. Depiction of calculated HOMO (1a) and LUMO (1b) of **1**, calculated HOMO (2a) and LUMO (2b) of **2**. HOMO-LUMO gap of **1** is calculated at 340 kJ/mol, and 325 kJ/mol for **2**, hydrogens are omitted for clarity and the isovalue is set at 0.05.

Compounds **1-3** were also characterized by IR spectroscopy. The IR spectrum of **1**

displayed a similar pattern to that of the corresponding complex, (Ph₃PAu)Mn(CO)₅ (1961(vs) cm⁻¹, 2062(s) cm⁻¹).⁵⁰ The IR spectrum of **1** showed two vibrational modes of the carbonyl groups, A₁ (1958(s) cm⁻¹), and E (2060(m) cm⁻¹), which correspond to axial and equatorial CO stretching modes, respectively. The 4-band (2A₁+B₁+B₂) pattern in the IR spectrum of **2** is similar to what was reported for (NHC)Al(Br)[(Fe(CO)₄)]⁵¹ (NHC = N-heterocyclic carbene) and cis-Fe(CO)₄(SnR₃)₂.⁵² CO stretching frequencies of **1** were calculated to be 1974 cm⁻¹ for axial, 1975 cm⁻¹ for equatorial, and 2055 cm⁻¹ for axial + equatorial. CO stretching frequencies of **2** were calculated to be 1893 cm⁻¹, 1921 cm⁻¹, 1967 cm⁻¹, and 2008 cm⁻¹. The IR spectrum of **3** showed similarities with the calculated (BP86) vibrational frequencies of the theoretical

Table 2. Selected spectroscopic data for **1-3**.

	1 (M = Mn)	2 (M = Fe)	3 (M = Co)
UV-vis (nm) ^a	332, 671	341, 505, 641	368
IR($\tilde{\nu}_{\text{CO}}$) cm ⁻¹	1958(s), 2060(m)	1889(m), 1958(m), 2005(m), 2041(w)	1820(m), 1849(m), 1948(m), 1972(s), 2008(m), 2035(m).
¹³ C NMR (CO) (ppm) ^b	210.94, 282.93	295.48	213.17
²⁰⁷ Pb NMR (ppm) ^c	8007.2	-	9010.4

a. UV-vis spectra were collected in hexanes at 298K. b. ¹³C{¹H} NMR spectra were

collected in C₆D₆ at 298K. c. ²⁰⁷Pb{¹H} NMR spectra were collected in C₆D₆ at 298K. butterfly complex Co₄(CO)₁₁, where the vibrational frequencies have relatively low wavenumber values of 1820 cm⁻¹ and 1849 cm⁻¹, which can be attributed to the bridging carbonyl groups, and that 2008(m) cm⁻¹ and 2035(m) cm⁻¹ to the terminal carbonyl groups(2020(s), 2026(s), 2032(s)).⁴²

Conclusion

In conclusion, the syntheses and characterizations of complexes Mn(CO)₅(PbAr^{iPr6}) (**1**), Fe(CO)₄(PbAr^{iPr6})₂ (**2**), Co₄(CO)₉(PbAr^{iPr6})₂ (**3**), have been described. They are rare examples of complexes synthesized by interaction of group 14 dimetallene and dinuclear transition metal carbonyls. The reactivities of diplumbyne and dinuclear metal carbonyls can be attributed to the charge-shift bond character of Pb≡Pb triple bond and M-M single bond. The syntheses of **1-3** are postulated to proceed via the reactions of Ar^{iPr6}Pb• radical fragment from the dissociation of Ar^{iPr6}PbPbAr^{iPr6} with Mn₂(CO)₁₀, Fe₂(CO)₉, or Co₂(CO)₈. Further studies of these synthesized metalloplumbylenes with small molecules are currently underway.

ASSOCIATED CONTENT

Supporting Information

The Supporting Information is available free of charge on the ACS Publications website at <https://pubs.acs.org/doi/10.1021/acs.organomet.xxxxxxx>.

Synthetic details for Na[Mn(CO)₅], Computational details, NMR, IR and electronic spectra of the described compounds (PDF)

Crystal data for CCDC 2018923 (CIF)

Crystal data for CCDC 2018925 (CIF)

Crystal data for CCDC 2027035 (CIF)

Optimized Cartesian coordinates (XYZ)

Accession Codes

CCDC 2018923, 2018925, 2027035 contain the supplementary crystallographic data for this paper. These data can be obtained free of charge via www.ccdc.cam.ac.uk/data_request/cif, or by emailing data_request@ccdc.cam.ac.uk, or by contacting The Cambridge Crystallographic Data Centre, 12 Union Road, Cambridge CB2 1EZ, UK; fax: +44 1223 336033.

AUTHOR INFORMATION

Corresponding Author

Philip P. Power – *Department of Chemistry, University of California, Davis, California 95616, United States;*
orcid.org/0000-0002-6262-3209; Email: pppower@ucdavis.edu

Authors

Qihao Zhu – *Department of Chemistry, University of California, Davis, California 95616, United States;*
orcid.org/0000-0002-5566-4491

Petra Vasko – *Department of Chemistry, Nanoscience Center, University of Jyväskylä, P.O. Box 35, FI-40014 University of Jyväskylä, Finland;*
orcid.org/0000-0003-4202-6869

James C. Fetting – *Department of Chemistry, University of California, Davis, California 95616, United States;*
orcid.org/0000-0002-6428-4909

Notes

The authors declare no competing financial interest.

ACKNOWLEDGMENTS

We are grateful to the National Science Foundation (NSF) for financial support (Grants CHE-1565501) and for the dual-source X-ray diffractometer (Grant 0840444). PV

would like to thank the Academy of Finland (project number 314794) and Prof. Heikki M. Tuononen for providing computational resources.

References

1. Fischer, E. O., On the Way to Carbene and Carbyne Complexes. *Advances in Organometallic Chemistry*, 14; Elsevier: Burlington, 1976; pp 1-32.
2. Marks, T. J., Dialkylgermylene- and -stannylene-pentacarbonylchromium complexes. *J. Am. Chem. Soc.* **1971**, 93, 7090-7091.
3. Cotton, J. D.; Davison, P. J.; Goldberg, D. E.; Lappert, M. F.; Thomas, K. M., Co-ordination chemistry of heavy-atom group IV donors, and the crystal and molecular structure of $[(\text{Me}_3\text{Si})_2\text{CH}]_2\text{SnCr}(\text{CO})_5$. *J. Chem. Soc., Chem. Commun.* **1974**, 893-895.
4. Petz, W., Transition-metal complexes with derivatives of divalent silicon, germanium, tin, and lead as ligands. *Chem. Rev.* **1986**, 86, 1019-1047.
5. Hashimoto, H.; Tobita, H., Recent advances in the chemistry of transition metal–silicon/germanium triple-bonded complexes. *Coord. Chem. Rev.* **2018**, 355, 362-379.
6. Álvarez-Rodríguez, L.; Cabeza, J. A.; García-Álvarez, P.; Polo, D., The transition-metal chemistry of amidinatosilylenes, -germylenes and -stannylens. *Coord. Chem. Rev.* **2015**, 300, 1-28.
7. Jutzi, P.; Leue, C., (Supermesityl)chlorogermylene (Supermesityl = $\text{Mes}^* = 2,4,6\text{-tBu}_3\text{C}_6\text{H}_2$): Synthesis and Derivatization to (Supermesityl)ferriogermynes. *Organometallics* **1994**, 13, 2898-2899.
8. Eichler, B. E.; Phillips, A. D.; Haubrich, S. T.; Mork, B. V.; Power, P. P., Synthesis, Structures, and Spectroscopy of the Metallostannylens $(\eta^5\text{-C}_5\text{H}_5)(\text{CO})_3\text{M-Sn-C}_6\text{H}_3\text{-2,6-Ar}_2$ (M = Cr, Mo, W; Ar = $\text{C}_6\text{H}_2\text{-2,4,6-Me}_3$, $\text{C}_6\text{H}_2\text{-2,4,6-Pr}_3$). *Organometallics* **2002**, 21, 5622-5627.
9. Pu, L.; Power, P. P.; Boltes, I.; Herbst-Irmer, R., Synthesis and Characterization of the Metalloplumbylenes $(\eta^5\text{-C}_5\text{H}_5)(\text{CO})_3\text{M-Pb-C}_6\text{H}_3\text{-2,6-Trip}_2$ (M = Cr, Mo, or W; Trip = $\text{-C}_6\text{H}_2\text{-2,4,6-i-Pr}_3$). *Organometallics* **2000**, 19, 352-356.
10. Lei, H.; Guo, J.-D.; Fettingner, J. C.; Nagase, S.; Power, P. P., Synthesis, Characterization, and CO Elimination of Ferrio-Substituted Two-Coordinate Germylenes and Stannylens. *Organometallics* **2011**, 30, 6316-6322.
11. Simons, R. S.; Power, P. P., $(\eta^5\text{-C}_5\text{H}_5)(\text{CO})_2\text{MoGeC}_6\text{H}_3\text{-2,6-Mes}_2$: A Transition-Metal Germylene Complex. *J. Am. Chem. Soc.* **1996**, 118, 11966-11967.
12. Pu, L.; Twamley, B.; Haubrich, S. T.; Olmstead, M. M.; Mork, B. V.; Simons, R. S.; Power, P. P., Triple Bonding to Germanium: Characterization of the Transition Metal Germylenes $(\eta^5\text{-C}_5\text{H}_5)(\text{CO})_2\text{M}:\text{Ge-C}_6\text{H}_3\text{-2,6-Mes}_2$ (M = Mo, W; Mes = $\text{-C}_6\text{H}_2\text{-2,4,6-Me}_3$) and $(\eta^5\text{-C}_5\text{H}_5)(\text{CO})_2\text{M}:\text{Ge-C}_6\text{H}_3\text{-2,6-Trip}_2$ (M = Cr, Mo, W; Trip = $\text{-C}_6\text{H}_2\text{-2,4,6-i-Pr}_3$) and the Related Single Bonded Metallogermynes $(\eta^5\text{-C}_5\text{H}_5)(\text{CO})_3\text{M-Ge-C}_6\text{H}_3\text{-2,6-Trip}_2$ (M = Cr, W). *J. Am. Chem. Soc.* **2000**, 122, 650-656.
13. Filippou, A. C.; Philippopoulos, A. I.; Portius, P.; Neumann, D. U., Synthesis and Structure of the Germylene Complexes $\text{trans-[X(dppe)}_2\text{W}\equiv\text{Ge}(\eta^1\text{-Cp}^*)]$ (X=Cl, Br, I) and Comparison of the $\text{W}\equiv\text{E}$ Bonds (E=C, Ge) by Density Functional Calculations. *Angew. Chem. Int. Ed.* **2000**, 39, 2778-2781.
14. Filippou, A. C.; Portius, P.; Philippopoulos, A. I.; Rohde, H., Triple Bonding to Tin: Synthesis and Characterization of the Stannylyne Complex $\text{trans-[Cl(PMe}_3)_4\text{W}\equiv\text{Sn-C}_6\text{H}_3\text{-2,6-Mes}_2]$. *Angew. Chem. Int. Ed.* **2003**, 42, 445-447.
15. Filippou, A. C.; Weidemann, N.; Schnakenburg, G.; Rohde, H.; Philippopoulos, A. I., Tungsten–

Lead Triple Bonds: Syntheses, Structures, and Coordination Chemistry of the Plumbylidyne Complexes $\text{trans-[X(PMe}_3)_4\text{W}\equiv\text{Pb(2,6-Trip}_2\text{C}_6\text{H}_3)]$. *Angew. Chem. Int. Ed.* **2004**, *43*, 6512-6516.

16. Queen, J. D.; Phung, A. C.; Caputo, C. A.; Fettingner, J. C.; Power, P. P., Metathetical Exchange between Metal-Metal Triple Bonds. *J. Am. Chem. Soc.* **2020**, *142*, 2233-2237.

17. Stender, M.; Phillips, A. D.; Wright, R. J.; Power, P. P., Synthesis and Characterization of a Digermanium Analogue of an Alkyne. *Angew. Chem. Int. Ed.* **2002**, *41*, 1785-1787.

18. Phillips, A. D.; Wright, R. J.; Olmstead, M. M.; Power, P. P., Synthesis and Characterization of 2,6-Dipp₂-H₃C₆SnSnC₆H₃-2,6-Dipp₂ (Dipp = C₆H₃-2,6-*i*-Pr₂): A Tin Analogue of an Alkyne. *J. Am. Chem. Soc.* **2002**, *124*, 5930-5931.

19. Pu, L.; Twamley, B.; Power, P. P., Synthesis and Characterization of 2,6-Trip₂H₃C₆PbPbC₆H₃-2,6-Trip₂ (Trip = C₆H₂-2,4,6-*i*-Pr₃): A Stable Heavier Group 14 Element Analogue of an Alkyne. *J. Am. Chem. Soc.* **2000**, *122*, 3524-3525.

20. McCrea-Hendrick, M. L.; Caputo, C. A.; Linnera, J.; Vasko, P.; Weinstein, C. M.; Fettingner, J. C.; Tuononen, H. M.; Power, P. P., Cleavage of Ge–Ge and Sn–Sn Triple Bonds in Heavy Group 14 Element Alkyne Analogues (EAr^{*i*Pr}₄)₂ (E = Ge, Sn; Ar^{*i*Pr}₄ = C₆H₃-2,6-(C₆H₃-2,6-*i*-Pr₂)₂) by Reaction with Group 6 Carbonyls. *Organometallics* **2016**, *35*, 2759-2767.

21. Pangborn, A. B.; Giardello, M. A.; Grubbs, R. H.; Rosen, R. K.; Timmers, F. J., Safe and Convenient Procedure for Solvent Purification. *Organometallics* **1996**, *15*, 1518-1520.

22. Queen, J. D.; Bursch, M.; Seibert, J.; Maurer, L. R.; Ellis, B. D.; Fettingner, J. C.; Grimme, S.; Power, P. P., Isolation and Computational Studies of a Series of Terphenyl Substituted Diplumbynes with Ligand Dependent Lead–Lead Multiple-Bonding Character. *J. Am. Chem. Soc.* **2019**, *141*, 14370-14383.

23. King R. B., Stone F. G. A., Sodium Salts of Carbonyl Hydrides Prepared in Ethereal Media. In *Inorg. Synth.*; McGraw-Hill book: New-York, 1963; Vol. 7, pp 196-201.

24. Reimer, K. J., Shaver, A., Quick, M.H. and Angelici, R.J., Pentacarbonylmanganese Halides. In *Inorg. Synth.*, Reagents for Transition Metal Complex and Organometallic Syntheses; Wiley-Interscience: Hoboken, 2006; pp 154-159.

25. Hicks, J.; Juckel, M.; Paparo, A.; Dange, D.; Jones, C., Multigram Syntheses of Magnesium(I) Compounds Using Alkali Metal Halide Supported Alkali Metals as Dispersible Reducing Agents. *Organometallics* **2018**, *37*, 4810-4813.

26. Lai, T. Y.; Tao, L.; Britt, R. D.; Power, P. P., Reversible Sn–Sn Triple Bond Dissociation in a Distannyne: Support for Charge-Shift Bonding Character. *J. Am. Chem. Soc.* **2019**, *141*, 12527-12530.

27. Joy, J.; Danovich, D.; Kaupp, M.; Shaik, S., Covalent vs Charge-Shift Nature of the Metal–Metal Bond in Transition Metal Complexes: A Unified Understanding. *J. Am. Chem. Soc.* **2020**, *142*, 12277-12287.

28. Goodman, J. L.; Peters, K. S.; Vaida, V., The determination of the manganese-manganese bond strength in Mn₂(CO)₁₀ using pulsed time-resolved photoacoustic calorimetry. *Organometallics* **1986**, *5*, 815-816.

29. Pan, S.; Zhao, L.; Dias, H. V. R.; Frenking, G., Bonding in Binuclear Carbonyl Complexes M₂(CO)₉ (M = Fe, Ru, Os). *Inorg. Chem.* **2018**, *57*, 7780-7791.

30. Wolf, S.; Fenske, D.; Kloppe, W.; Feldmann, C., [Pb{Mn(CO)₅}₃][AlCl₄]: a lead-manganese carbonyl with AlCl₄-linked PbMn₃ clusters. *Dalton Trans.* **2019**, *48*, 4696-4701.

31. Braunschweig, H.; Damme, A.; Dewhurst, R. D.; Kramer, T.; Östreicher, S.; Radacki, K.; Vargas, A., Ditopic Ambiphilicity of an Anionic Dimetalloborylene Complex. *J. Am. Chem. Soc.* **2013**, *135*, 2313-2320.

32. Clementi, E.; Raimondi, D. L.; Reinhardt, W. P., Atomic Screening Constants from SCF Functions. II. Atoms with 37 to 86 Electrons. *J. Chem. Phys.* **1967**, *47*, 1300-1307.
33. Pyykkö, P.; Atsumi, M., Molecular Single-Bond Covalent Radii for Elements 1–118. *Chem. Eur. J.* **2009**, *15*, 186-197.
34. Cordero, B.; Gómez, V.; Platero-Prats, A. E.; Revés, M.; Echeverría, J.; Cremades, E.; Barragán, F.; Alvarez, S., Covalent radii revisited. *Dalton Trans.* **2008**, 2832-2838.
35. Herberhold, M.; Tröbs, V.; Milius, W.; Wrackmeyer, B., Carbonyliron-Lead Complexes: Multinuclear Magnetic Resonance Study in Solution and X-Ray Structure Determination of $[\text{Et}_2\text{PbFe}(\text{CO})_4]_2$. *Z. Naturforsch. B* **1994**, *49*, 1781.
36. Wade, K., The structural significance of the number of skeletal bonding electron-pairs in carboranes, the higher boranes and borane anions, and various transition-metal carbonyl cluster compounds. *J. Chem. Soc. D* **1971**, 792-793.
37. Mingos, D. M. P., A General Theory for Cluster and Ring Compounds of the Main Group and Transition Elements. *Nat. Phys.* **1972**, *236*, 99-102.
38. Wei, C. H., Structural analyses of tetracobalt dodecacarbonyl and tetrarhodium dodecacarbonyl. Crystallographic treatments of a disordered structure and a twinned composite. *Inorg. Chem.* **1969**, *8*, 2384-2397.
39. Plečnik, C. E.; Liu, S.; Chen, X.; Meyers, E. A.; Shore, S. G., Lanthanide–Transition-Metal Carbonyl Complexes: New $[\text{Co}_4(\text{CO})_{11}]^{2-}$ Clusters and Lanthanide(II) Isocarbonyl Polymeric Arrays. *J. Am. Chem. Soc.* **2004**, *126*, 204-213.
40. Chini, P., The closed metal carbonyl clusters. *Inorg. Chim. Acta* **1968**, *2*, 31-51.
41. Farrugia, L. J.; Braga, D.; Grepioni, F., A structural redetermination of $\text{Co}_4(\text{CO})_{12}$: evidence for dynamic disorder and the pathway of metal atom migration in the crystalline phase. *J. Organomet. Chem.* **1999**, *573*, 60-66.
42. Zhang, X.; Li, Q.-s.; Xie, Y.; King, R. B.; Schaefer, H. F., A Carbonyl Group Bridging Four Metal Atoms in a Homoleptic Carbonylmatal Cluster: The Remarkable Case of $-\text{Co}_4(\text{CO})_{11}$. *Eur. J. Inorg. Chem.* **2008**, 2158-2164.
43. Simons, R. S.; Pu, L.; Olmstead, M. M.; Power, P. P., Synthesis and Characterization of the Monomeric Diaryls $\text{M}\{\text{C}_6\text{H}_3\text{-2,6-Mes}_2\}_2$ (M = Ge, Sn, or Pb; Mes = 2,4,6-Me₃C₆H₂–) and Dimeric Aryl–Metal Chlorides $[\text{M}(\text{Cl})\{\text{C}_6\text{H}_3\text{-2,6-Mes}_2\}]_2$ (M = Ge or Sn). *Organometallics* **1997**, *16*, 1920-1925.
44. Kano, N.; Tokitoh, N.; Okazaki, R., Synthesis and X-ray Crystal Structure of Bis{2,4,6-tris[bis(trimethylsilyl)methyl]phenyl}dibromoplumbane: The First Monomeric Diorganodihaloplumbane in the Crystalline State. *Organometallics* **1997**, *16*, 2748-2750.
45. McCrea-Hendrick, M.; Bursch, M.; Gullett, K.; Maurer, L.; Fettingner, J.; Grimme, S.; Power, P., Counterintuitive Interligand Angles in the Diaryls $\text{E}\{\text{C}_6\text{H}_3\text{-2,6-(C}_6\text{H}_2\text{-2,4,6- iPr}_3\text{)}_2\}_2$ (E = Ge, Sn, or Pb) and Related Species: The Role of London Dispersion Forces. *Organometallics* **2018**, *37*.
46. Elschenbroich, C., *Organometallic*. Wiley-VCH: Weinheim, 2006; pp. 356-372.
47. Aime, S.; Gobetto, R.; Osella, D.; Milonej, L.; Hawkes, G. E.; Randall, E. W., Reinvestigation of the solution structure of $\text{Co}_4(\text{CO})_{12}$ by ^{13}C and ^{59}Co NMR. 2. *J. Magn. Reson. (1969)* **1985**, *65*, 308-315.
48. Richert, T.; Elbayed, K.; Raya, J.; Granger, P.; Braunstein, P.; Rosé, J., ^{59}Co NMR in Tetrahedral Clusters. *Magn. Reson. Chem.* **1996**, *34*, 689-696.
49. Friedel, R. A.; Wender, I.; Shufler, S. L.; Sternberg, H. W., Spectra and Structures of Cobalt Carbonyls1. *J. Am. Chem. Soc.* **1955**, *77*, 3951-3958.
50. Coffey, C. E.; Lewis, J.; Nyholm, R. S., 339. Metal–metal bonds. Part I. Compounds of gold(0)

with the carbonyls of manganese, iron, and cobalt. *J. Chem. Soc.* **1964**, 1741-1749.

51. Tan, G.; Szilvási, T.; Inoue, S.; Blom, B.; Driess, M., An Elusive Hydridoaluminum(I) Complex for Facile C–H and C–O Bond Activation of Ethers and Access to Its Isolable Hydridogallium(I) Analogue: Syntheses, Structures, and Theoretical Studies. *J. Am. Chem. Soc.* **2014**, *136*, 9732-9742.

52. Pomeroy, R. K.; Vancea, L.; Calhoun, H. P.; Graham, W. A. G., Stereochemically nonrigid six-coordinate metal carbonyl complexes. 3. The series $\text{cis-Fe}(\text{CO})_4(\text{SnR}_3)_2$ (R = methyl, ethyl, propyl, butyl, phenyl, chloro) and the x-ray structure of tetracarbonylbis(triphenylstannyl)iron(II). *Inorg. Chem.* **1977**, *16*, 1508-1514.

For Table of Contents

